IEEE Access
Multidisciplinary | Rapid Review | Open Access Journal

Received March 23, 2018, accepted April 20, 2018, date of publication April 25, 2018, date of current version May 16, 2018.

Digital Object Identifier 10.1109/ACCESS.2018.2829897

Performance Analysis of IEEE 802.11p Safety Message Broadcast With and Without Relaying at Road Intersection

MD. NOOR-A-RAHIM[1], G. G. MD. NAWAZ ALI[2], HIEU NGUYEN[1], AND YONG LIANG GUAN[1]

[1]School of Electrical and Electronic Engineering, Nanyang Technological University, Singapore 639798
[2]Department of Automotive Engineering, Clemson University, Clemson, SC 29634, USA

Corresponding author: Md. Noor-A-Rahim (narahim@ntu.edu.sg)

This work was supported by the NTU-NXP Intelligent Transport System Test-Bed Living Laboratory Fund through the Economic Development Board, Singapore, under Grant S15-1105-RF-LLF.

ABSTRACT Dedicated short-range communication (DSRC), which is an essential part of vehicle-to-vehicle/infrastructure communication to enhance the road safety, is often characterized by the IEEE 802.11p standard. Numerous works have been done on the DSRC safety message broadcasting performance for highway scenario. However, up to date, no work has been done on the performance of the IEEE 802.11p safety message broadcasting for the road-intersection scenario in urban environment. An intersection scenario is different from a highway scenario. In a highway scenario, it is often been considered that all the vehicles have the same communication range as well as the same carrier sensing range. However, this is not the case for the intersection scenario, where there exist a lot of obstructions, such as buildings and urban canyons. In an intersection, the communication and carrier sensing ranges of a vehicle heavily depend on the location of that vehicle. This paper first analyzes and then provides solution on improving the broadcasting performance of the DSRC safety message at an intersection while considering the IEEE 802.11p enhanced distributed channel access mechanism. To facilitate different communication and carrier sensing ranges of different vehicles, we divide the intersection region into few parts/areas based on an empirically validated path loss model. We present an analytical study on the packet reception rates and channel access delay which is applicable for the different positions of transmitters and receivers in the intersection areas. The analytical results are verified by the NS-3 simulation. From the results, we find that the overall delivery ratio is very poor when the broadcasting vehicle is not close enough to the intersection-center. To improve the overall broadcast performance of such scenarios, we employ a road side unit (RSU) at the intersection-center to relay the safety messages once. We show the performance improvement via relaying while first using omni-directional and then using special sector antennas, the so-called bidirectional antenna, at the RSU. From the results, it is shown that relaying with the omni-directional antenna gives moderate improvement on the overall delivery ratio, while a significant improvement can be achieved by relaying with sector antenna.

INDEX TERMS IEEE 802.11p, V2X communication, intelligent transport systems, DSRC.

I. INTRODUCTION

Vehicle-to-vehicle (V2V) communication plays an important role in intelligent transport systems (ITS). A vehicle equipped with a DSRC unit based on IEEE 802.11p standard [1], can communicate with other vehicles to exchange warning messages for avoiding accident and improving traffic situation. The safety messages, such as Cooperative Awareness Message (CAM) [2] or Basic Safety Message (BSM) [3], contain a vehicle's instantaneous maneuvering information (such as location, speed, heading etc.) based on the on-board Global Navigation Satellite System (e.g., GPS device) as well as other information such as vehicle type, breaks condition etc. When a vehicle receives the safety messages from other neighboring vehicles, a suitable audio/visual warning may be displayed to help the driver to enhance driving safety and comfort. The capability of receiving the safety message is

important in a dense vehicular communication network with many vehicles attempting to broadcast the safety messages in an uncoordinated way.

A lot of works, such as [4]–[17], have been previously done on the performance analysis of IEEE 802.11 MAC protocol. Among them, [4]–[9] analyzed the IEEE 802.11 MAC protocol for general adhoc networks, while [10]–[17] specifically addressed the performance analysis of IEEE 802.11p EDCA (Enhanced Distributed Channel Access) for vehicular communication. In all of these works, it is assumed that all the nodes in the region of interest have the same communication range as well as the same carrier sensing range. This assumption is reasonable for the highway scenario, where there exist line-of-sight (LOS) communication links among all the vehicles. However, an urban traffic intersection scenario is different from a highway scenario, since there exist a lot of obstructions, such as buildings, urban canyons etc. in the former but not in the latter. In an intersection scenario, it is expected that a vehicle close to the intersection-center will have longer ranges along the perpendicular street than vehicles that are further away from the intersection-center. Thus, the assumption of having same communication and carrier sensing ranges for all vehicles is not valid for intersection environment. Such assumption in intersection scenario will result in incorrect performance analysis of IEEE 802.11p standard. Thus, a proper analysis of the IEEE 802.11p standard for intersection scenario, which incorporates the heterogeneous nature of communication and carrier sensing ranges depending on the vehicles' positions, is necessary. Few works, such as [18]–[21], investigated performance analysis of safety message broadcasting for intersection scenario. However, they also assumed the same communication and carrier sensing ranges for all vehicles, which is not correct. Moreover, none of this works [18]–[21] considered the IEEE 802.11p EDCA mechanism in the broadcasting performance analysis.

In this paper, we study the broadcasting performance of DSRC safety message at a road intersection. To the best of our knowledge, this is the first work that deals with the broadcasting performance at the intersection while considering the IEEE 802.11p EDCA mechanism with heterogeneous communication and carrier sensing ranges. Based on practical path loss model, we divide the intersection region into several parts to incorporate the impact of different communication and carrier sensing ranges. The packet reception rates at different areas are shown when the transmitting vehicle resides in a particular area. An analytical model on the overall packet delivery ratio and average access delay is presented while considering different transmitters' positions. The numerical results reveal that the message delivery ratio is not high for the transmitting vehicles, which are not close to the intersection-center. To improve the message delivery ratio, we propose to relay (rebroadcast) the message through a dedicated RSU, placed at the center of the intersection. The relaying is firstly shown with omni-directional at RSU and then with bidirectional sector antennas at RSU. The results show that relaying with omni-directional antenna provides moderate gain in packet delivery ratio, while relaying with sector antenna improves that gain significantly. The realistic simulation performed in NS-3 supports the analytical results.

The remainder of this paper is organized as follows. In Section II, we demonstrate the overview of an intersection and a brief overview of IEEE 802.11p standard. In Section III, we approximate the communication and carrier sensing ranges of different areas by partitioning the intersection based on a path loss model. In Section IV, we analyze the delivery ratio and average access delay for different parts of the intersection. Simulation results and discussions on the safety message reception rate and average access delay are presented in Section V. Considering two different antenna configurations at RSU, the performance improvement through RSU relaying is investigated in Section VI.

II. PRELIMINARIES

In this section, we present the road-intersection model, a brief overview of IEEE 802.11p EDCA mechanism and causes of packet loss. Major notations, used in this paper, are summarized in Table 1.

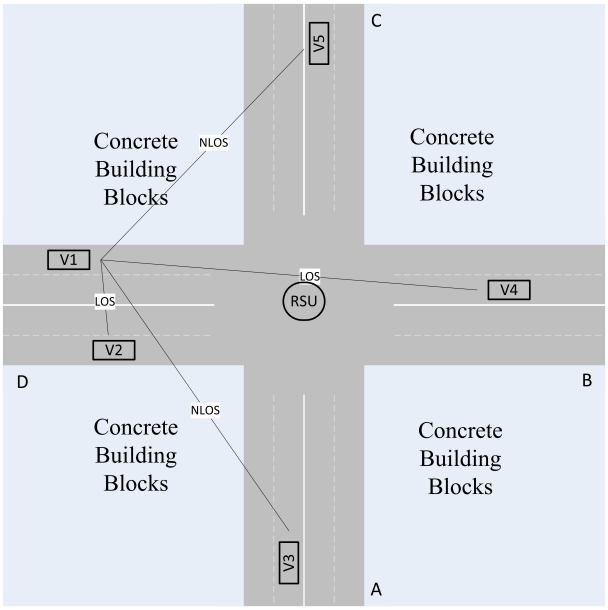

FIGURE 1. V2X communication at an intersection.

A. INTERSECTION MODEL

A typical intersection scenario, consists of four branches (A, B, C, and D) is depicted in Fig. 1. In the figure, the characteristics of the communication links are shown for the case where a vehicle V1 communicates with other vehicles. For two vehicles on the same street, one can say that the communication link between them is typically line-of-sight (LOS) because the transmitted signal can reach from one to another through a direct transmission path. However

TABLE 1. Major notations used in the paper.

Notation	Definition
AC[j]	Access category j, $j \in \{0, 1, 2, 3\}$
AIFSN[j]	Arbitration inter-frame space number of AC[j]
$CW_{\min}[j]$	Minimum contention window size of AC[j]
$CW_{\max}[j]$	Maximum contention window of AC[j]
SIFS	Short inter-frame space
t_s	Slot time
$W_\ell[j]$	Contention window size of AC[j] at ℓ^{th} back-off stage
$M[j]$	Maximum times the contention window of AC[j] can be doubled
$L[j]$	retry limit for AC[j]
P_{TX}	Transmit power
P_{RX}	Receive power
d_t	Distance of transmitter to the intersection-centre
d_r	Distance of receiver to the intersection-centre
w_r	Street width of receiver
d_w	Distance of transmitter to wall
d_b	Critical distance
X_σ	Fading parameter
λ	Wave length
n_{NLOS}	Path loss exponent
i_s	Environment parameter (1 for suburban environment and 0 for urban)
V_{Tx}	Transmitting vehicle
$\mathcal{Z}$	Set of areas, $\mathcal{Z} = [A_3, A_2, A_1, G, B_1, B_2, B_3]$
PRP	Packet reception probability
N_k	Number of vehicle at area $k \in \mathcal{Z}$
p_{t_k}	Overall transmission probability of a vehicle at area k
T_r	Packet transmission time
$p_{e_k}[j]$	Transmission probability of a packet of AC[j] at area k
$p_{i_k}[j]$	Internal transmission probability of AC[j] at area k
$p_{v_k}[j]$	Internal collision probability of AC[j] at area k
$p_{b_k}[j]$	Back-off probability of AC[j] at area k
$p_a[j]$	Arrival probability of a packet of AC[j]
$\Lambda[j]$	Packet arrival rate (packets/sec) for AC[j].
$\rho_k[j]$	Probability that at least one packet of AC[j] is available for transmission at area k
$D_k[j]$	Average access delay of AC[j] at area k
ODR	overall packet delivery ratio
RPRP	Packet reception probability after relaying

if they are on the different streets, the radio link may be non-line-of-sight (NLOS) and thus tends to be unreliable. For instance, in Fig. 1, the communication link between V1 and V2 (or V4) is LOS, whereas the link between V1 and V3 (or V5) is NLOS. For a generalized setting, similar to Fig. 1, we will analyze the communication and carrier sensing ranges of different parts of intersection in Section III. Note that a road side unit (RSU) is also depicted in Fig. 1, and the relaying performance through RSU will be analyzed in Section VI.

B. OVERVIEW OF IEEE 802.11p EDCA MECHANISM

The IEEE 802.11p EDCA mechanism allows four access categories (namely AC[0], AC[1], AC[2], and AC[3]) in a vehicle with different priorities. The priority level and parameters used for each AC are summarized in Table 2. In the table, AIFSN[j], $CW_{\min}[j]$ and $CW_{\max}[j]$ corresponds to the arbitration inter-frame space number, minimum contention window and maximum contention window of AC[j], respectively, where $j \in \{0, 1, 2, 3\}$.

TABLE 2. IEEE 802.11p EDCA parameters for access categories.

AC[j]	Priority	$CW_{\min}[j]$	$CW_{\max}[j]$	AIFSN[j]
AC[0]	Highest	3	7	2
AC[1]	2^{nd} Highest	7	15	3
AC[2]	3^{rd} Highest	15	1024	6
AC[3]	Lowest	15	1024	9

Following [1], we now describe the key ideas of EDCA mechanism for a vehicle's perspective. Since each AC operates independently, internal collision may occur when two or more ACs try to access the same time slot. In the absence of internal collision each AC operates in the following manner. When a packet of AC[j] is available for transmission, the packet will be sent immediately if the channel is sensed idle and remains idle for a $T_A[j]$ time period. $T_A[j]$ is defined by $T_A[j] = \text{SIFS} + \text{AIFSN}[j] \times t_s$, where SIFS is the short inter-frame space and t_s is the duration of a slot time. If the channel is sensed busy, AC[j] will enter into back-off stage once the channel is sensed idle for a $T_A[j]$ time period. In the back-off stage, AC[j] starts it's back-off counter by setting an initial random value chosen from [0, $W_0[j]$], where $W_0[j] = CW_{\min}[j]$. Then if the channel is sensed idle for t_s time period, the counter is decreased by one. During back-off procedure, the counter will be frozen if the channel is sensed busy. The counter will be resumed once the channel is sensed idle continuously for a $T_A[j]$ time period. Finally, the packet will be sent as soon as the counter reaches at zero.

In the case of internal collision, the AC with the highest priority transmits and lower priority ACs enter back-off stage with contention window size of $W_\ell[j]$, where $W_\ell[j]$ is the contention window size at the ℓ^{th} back-off stage. This strategy is known as internal collision avoidance procedure. $W_\ell[j]$ is defined by following:

$$W_\ell[j] = \begin{cases} 2^\ell W_0[j], & \text{if } \ell \le M[j] \\ 2^{M[j]} W_0[j], & \text{if } M[j] < \ell \le L[j] \end{cases} \quad (1)$$

where $M[j] = \log_2 \frac{CW_{\max}[j]+1}{CW_{\min}[j]+1}$ and $L[j]$ is the retry limit for AC[j] in the case of internal collision. Note that no acknowledgement (ACK) frame is considered in this paper due to the broadcasting scenario.

C. CAUSES OF PACKET LOSS

Packet loss in vehicular communication mainly occurs due to the following two reasons: (i) Buildings/obstacles: The transmitted signal strength falls drastically when it gets obstructed by buildings or obstacles. Thus, buildings/obstacles induce packet drop due to the poor received signal strength at receiver. (ii) Packet collision/interference: Buildings/obstacles also induce the hidden node problem in

CSMA-CA scenario, where due to the loss of transmitted signal strength, some vehicles become unaware about the ongoing transmission and consider the channel as idle. This may cause multiple transmissions to occur at the same time, which result in packet collision at the receiver. Besides hidden node collision, packet collision may occur even when the transmitters are located in the carrier sensing region of each other. In this case, when multiple vehicles have packets to transmit and they start to sense the channel at the same time and choose the same back off instant, this will cause multiple transmissions to occur at exactly the same time and hence cause collision in the receiving vehicle.

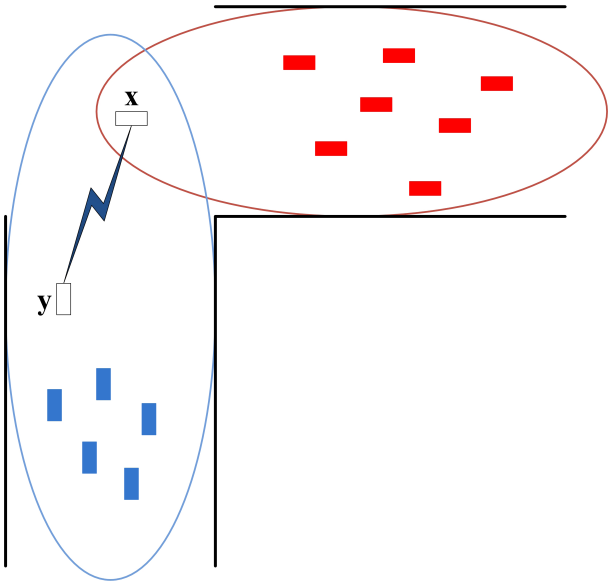

FIGURE 2. Illustration of a simple communication scenario (Tx: vehicle *y* and Rx: vehicle *x*) in the presence of interferer vehicles (blue colored) and hidden vehicles (red colored).

Considering the above factors, we now illustrate the packet reception probability by the following example. In Fig. 2, we consider two vehicles (x and y) and two groups of vehicles (colored as blue and red). For simplicity, we assume that all the blue vehicles and vehicle y have the same communication range (depicted by a blue eclipse). We also assume that all the red vehicles have the same communication range and their range is depicted by a red eclipse. We consider that vehicle x lies in the range of both groups and vehicle y. Assuming no path-loss between y and x, a successful transmission from y to x is only possible when no blue vehicle starts transmission exactly when y starts to transmit and no red vehicle starts transmission at the same as y. Thus, for y all the blue vehicles act as interferer nodes, while all the red vehicles act as hidden nodes. The packet reception probability (PRP) of x when y transmits is given by,

$$\text{PRP} = \text{RP}_{\text{loss}}(1 - p_{t_b})^{N_b} \times (1 - p_{t_h})^{\frac{2N_r T_r}{t_s}} \tag{3}$$

where RP_{loss} is the reception probability when there is no packet collision; N_b and N_r are the number of blue and red vehicles, respectively; p_{t_b}, p_{t_r} are the overall transmission probability of blue and red vehicles, respectively; T_r is the packet transmission time. RP_{loss} depends on the channel condition between transmitter and receiver. For ideal communication scenario, $\text{RP}_{\text{loss}} = 1$.

III. COMMUNICATION AND CARRIER SENSING RANGES AT INTERSECTION

In most of the previous works on ad-hoc networks (including [4]–[16], [22]), it is assumed that all nodes have the same communication range as well as carrier sensing range. However, this assumption is not valid in the case of road intersections. Instead, the communication and carrier sensing ranges vary depending on the position of the vehicle at the intersection. For instance, a vehicle close to the intersection-center will have longer ranges along the perpendicular street than vehicles that are further away from the intersection-center. Thus, depending on the vehicle's position, its corresponding hidden nodes varies. This practical and important aspect was not considered in the previous works [18]–[21]. Based on path loss and fading model for NLOS and LOS scenarios, in this section, we divide the intersection into segments to facilitate the different communication and carrier sensing ranges subject to the position of the transmitting vehicle. Based on the derived areas around the intersection, we will present the analysis of IEEE 802.11p standard in later sections.

The measurement-based model of path loss and fading for NLOS scenario at intersection has been well reported in [23]. In this model, the path loss depends on the street width, the distance of transmitter (Tx)/receiver (Rx) to the intersection-center, the distance of transmitter to the wall and the carrier frequency. The path-loss model, presented in [24] and [25], is shown in the bottom of this page (see eq. (2)), where d_t (d_r) denotes the distance of Tx (respectively, Rx) to the intersection-center, w_r is the width of Rx street, d_w is the distance of Tx to the wall, i_s is the environment parameter (1 for suburban environment and 0 for urban), d_b denotes the critical distance, λ is the wave length and n_{NLOS} is the path loss exponent. We model the small scale fading as Gaussian

$$PL_{\text{NLOS}} = 3.75 + i_s 2.94 + \begin{cases} 10\log_{10}\left(\left(\dfrac{d_t^{0.957}}{(d_w w_r)^{0.81}}\dfrac{4\pi d_r}{\lambda}\right)^{n_{\text{NLOS}}}\right), & \text{if } d_r \le d_b \\ 10\log_{10}\left(\left(\dfrac{d_t^{0.957}}{(d_w w_r)^{0.81}}\dfrac{4\pi d_r^2}{\lambda d_b}\right)^{n_{\text{NLOS}}}\right), & \text{if } d_r > d_b \end{cases} \tag{2}$$

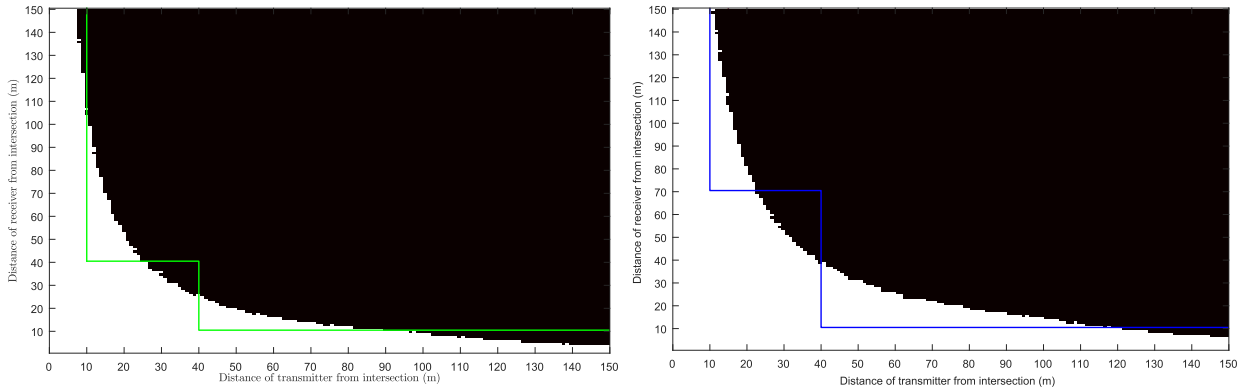

(a) (b)

FIGURE 3. Communication and carrier sensing regions at the intersection. The white area represents the case when the average received signal strength is greater than the respective threshold, while the dark area represents the case when the signal strength is less than or equal to the threshold. An approximation of the communication region is shown though a green line, while an approximation of the carrier sensing region is shown though a blue line. (a) Communication region at intersection. (b) Carrier sensing region at intersection.

random variable, denoted by X_σ, with zero mean with standard deviation of $\sigma = 4.1$dB. Based on eq. (2) as well as the fading parameter X_σ, the combination of path loss and fading in the form of $PL_{\text{NLOS}}^{\text{fading}}$ can be written as,

$$PL_{\text{NLOS}}^{\text{fading}} = \alpha_{\text{NLOS}} + 10n_{\text{NLOS}} \log_{10}(\beta_{N\text{NLOS}} d_t^{n_t} d_r^{n_r}) + X_\sigma, \tag{4}$$

where $\alpha_{\text{NLOS}} = 3.75 + i_s 2.94$, $n_t = 0.957$, $\beta_{\text{NLOS}} = \frac{1}{(d_w w_r)^{0.81}} \frac{4\pi}{\lambda}$ or $\frac{1}{(d_w w_r)^{0.81}} \frac{4\pi}{\lambda d_b}$ and $n_r = 1$ or 2 according to $d_r \leq d_b$ or $d_r > d_b$, respectively. Assuming the transmit power is P_{TX}, then received signal power can be expressed as,

$$\begin{aligned} P_{\text{RX}} &= P_{\text{TX}} - PL_{\text{NLOS}}^{\text{fading}} \\ &= P_{\text{TX}} - \alpha_{\text{NLOS}} - 10n_{\text{NLOS}} \log_{10}(\beta_{\text{NLOS}} d_t^{n_t} d_r^{n_r}) - X_\sigma. \end{aligned} \tag{5}$$

At the receiver, the received signal strength needs to be higher than a certain threshold to correctly decode the safety message. We refer to this threshold as communication threshold. Similarly, to identify the channel as busy, the received signal strength requires to be higher than another threshold, so called carrier sensing threshold. In this paper, we consider the thresholds for the communication and carrier sensing as -75 dBm and -85 dBm, respectively.

From the average received signal strength and the thresholds, we find the communication and carrier sensing regions at the intersection for NLOS scenario. In this paper, we consider an area of $300 \times 300\text{m}^2$ provided that the intersection-center is located at the middle of the area. The parameters used in the simulation are listed in Table 3. In Fig 3a and Fig 3b, we show the communication and carrier sensing regions, respectively, while varying the distance of transmitter/receiver from the intersection-center. In the simulation, we consider the transmitter/receiver position from 1m to 150m from the intersection-center with an interval of 1m.

TABLE 3. Simulation parameters.

Parameter	Value
Carrier Frequency	178 (5.89GHz)
Bandwidth	10MHz
Transmit power	23dBm
Antenna gain	3dB
Number of lane per street	6
Lane width	3m
RX street width	18m
Distance of TX to wall	5m
Critical distance d_b	100m
n_{NLOS}	2.69

To generate these figures, we calculate the received power for all possible pairs of transmitter and receiver positions. We repeat the process for 500 times and an average received power is calculated for each pair. The serrated nature of the curve is due to the fact that for a given transmitter position from the intersection-center the received power is always higher than the thresholds for a certain range of receiver positions. From the results, it is obvious that the communication and carrier sensing ranges change with the position of the transmitter. In analysis, it is not feasible to treat each transmitter position separately. For simplicity, we approximate the communication and carrier sensing regions such that the approximated regions closely match with the actual results while providing feasible number of partitions around the intersection.

In LOS environment, the path loss and fading model is a function of distance d between Tx and Rx instead of d_t and d_r (distances to the intersection-center) in NLOS scenario. From the LOS models, presented in [24], [25], it is observed that the average received signal strength is well above of -75 dBm regardless the distance between Tx and Rx for an area of $300 \times 300\text{m}^2$. From this observation and from the approximated communication and carrier sensing regions for NLOS

TABLE 4. Elements of $\mathcal{I}_{x,y}$ and $\mathcal{H}_{x,y}$.

y	when $x = A_2$ or $x = A_3$		when $x = A_1$		when $x = G$	
	$\mathcal{I}_{A_3,y}$	$\mathcal{H}_{A_3,y}$	$\mathcal{I}_{A_1,y}$	$\mathcal{H}_{A_1,y}$	$\mathcal{I}_{G,y}$	$\mathcal{H}_{G,y}$
A_3	$\{A_3, A_2, A_1, G\}$	$\{\}$	$\{A_3, A_2, A_1, G\}$	$\{\}$	$\{A_3, A_2, A_1, G\}$	$\{\}$
A_1 or A_2	$\{A_3, A_2, A_1, G\}$	$\{B_1\}$	$\{A_3, A_2, A_1, G, B_1\}$	$\{\}$	$\{A_3, A_2, A_1, G, B_1\}$	$\{\}$
G	$\{A_3, A_2, A_1, G\}$	$\{B1, B2, B3\}$	$\{A_3, A_2, A_1, G, B_1, B_2\}$	$\{B3\}$	$\{A_3, A_2, A_1, G, B_1, B_2, B_3\}$	$\{\}$
B_1	N/A	N/A	$\{A_1, G, B_1, B_2\}$	$\{B3\}$	$\{A_1, G, B_1, B_2, B_3\}$	$\{\}$
B_2	N/A	N/A	N/A	N/A	$\{A_1, G, B_1, B_2, B_3\}$	$\{\}$
B_3	N/A	N/A	N/A	N/A	$\{G, B_1, B_2, B_3\}$	$\{\}$

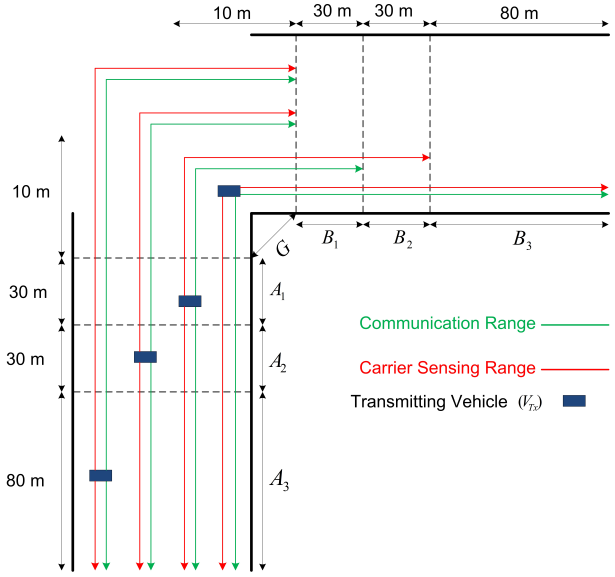

FIGURE 4. Partition at the intersection based on the approximate communication and carried sensing regions. The blue rectangular box represents the transmitting vehicle.

scenario, the resultant communication and carried sensing ranges for different areas are abstracted in Fig. 4.[1] Only two perpendicular branches are considered due to the symmetry of the intersection. From the approximations, we get seven areas/partitions ($A_3, A_2, A_1, G, B_1, B_2,$ and B_3) around the intersection. We assume that all vehicles in a particular partition have the same communication range as well as the same carrier sensing range. From transmission point of view, A_2 and A_3 (B_2 and B_3) are the same, since they have the same communication and carrier sensing ranges. From reception point of view, B_1 and B_2 (A_1 and A_2) are the same, since they have the same number of interferer vehicles. In the rest of the paper, we define a set $\mathcal{Z}$ as the set of partitions around the intersection, namely, $\mathcal{Z} = [A_3, A_2, A_1, G, B_1, B_2, B_3]$.

IV. PACKET RECEPTION PROBABILITY AND DELAY ANALYSIS

In the packet reception probability and delay analysis, we make following assumptions:

- We assume an ideal channel condition, which means that the receivers in the communication range can successfully decode a packet if no packet collision occurs.
- The vehicles are assumed to be stationary within the duration of one packet transmission.
- The interference from a signal with strength less than -85 dBm is neglected.
- The impact of the vehicles located outside the region of interest is neglected. In other words, we consider the impacts of the vehicles in an intersection area of 300×300 m^2 with the intersection-center located in the center of the area (i.e., the length of roads in each direction is 150 m from the intersection-center). We neglect the impact of vehicles beyond 150 m from the intersection-center as this paper focuses on the traffic intersection BSM broadcast effectiveness.
- The impact of packet drop due to the overflow of the queue is not considered.

Let PRP(x, y) is the packet reception probability of any vehicle at area y provided that the transmitting vehicle at area x, where $x, y \in \mathcal{Z}$. To find PRP(x, y), we introduce two sets for a transmitting vehicle at x and reception vehicle at y: $\mathcal{I}_{xy}$ and $\mathcal{H}_{xy}$, which are defined as follows,

- $\mathcal{I}_{xy}$ is the set of areas which vehicles can sense the transmission from transmitting vehicle at x and can cause collision at the receiving vehicles at y. We refer to the vehicles of $\mathcal{I}_{xy}$ as interferer vehicles.
- $\mathcal{H}_{xy}$ is the set of areas which vehicles cannot sense the transmission from transmitting vehicle at x but can cause collision at the receiving vehicles at y. We refer to the vehicles of $\mathcal{H}_{xy}$ as hidden vehicles.

We summarize $\mathcal{I}_{xy}$ and $\mathcal{H}_{xy}$ in Table 4, which are obtained from the communication and carrier sensing ranges shown in Fig. 4. According to the communication principle, a successful transmission from the transmitting vehicle at area x to any vehicle at y is only possible when no vehicle of $\mathcal{I}_{xy}$ transmits at the time slot when transmitting vehicle broadcasts and no vehicle of $\mathcal{H}_{xy}$ starts transmission at any time during transmitting vehicle broadcasts. Thus PRP(x, y) is defined as

$$\text{PRP}(x, y) = \prod_{q \in \mathcal{I}_{x,y}} (1 - p_{t_q})^{N_q} \prod_{\ell \in \mathcal{H}_{x,y}} (1 - p_{t_\ell})^{\frac{2N_\ell T_r}{t_s}}, \quad (6)$$

where N_k is the number of vehicle at area $k \in \mathcal{Z}$, p_{t_k} is the overall transmission probability of a vehicle at area k, and T_r is the packet transmission time. From the distribution of the vehicles along the streets, number of vehicles in any particular area can be obtained.

[1] Fig. 4 does not show true scale.

Now to find packet reception probability, we need to find p_{t_k}. This transmission probability depends on the parameters of the IEEE 802.11p standards, packet arrival rate and the number of vehicles, which carrier sensing ranges cover the transmitting vehicle. For any vehicle at area $k \in \mathcal{Z}$, the overall transmission probability p_{t_k} is given by

$$p_{t_k} = \sum_{\ell=0}^{3} p_{e_k}[\ell], \tag{7}$$

where $p_{e_k}[j]$ is the transmission probability of a packet of AC[j]. $p_{e_k}[j]$ is defined by

$$p_{e_k}[j] = \begin{cases} p_{i_k}[j], & \text{for } j = 0 \\ p_{i_k}[j] \prod_{\ell=0}^{j-1} (1 - p_{i_k}[\ell]), & \text{otherwise} \end{cases} \tag{8}$$

where $p_{i_k}[j]$ is the internal transmission probability of AC[j]. From the Markov chain model, shown in [15], we can derive following relationship (details are provided in the Appendix):

$$p_{i_k}[j] = \begin{cases} \dfrac{1}{\dfrac{W_0[j]+1}{2(1-p_{b_k}[j])} + \dfrac{1-\rho_k[0]}{p_a[j]}} & \text{for } j = 0 \\ \dfrac{1-p_{v_k}^{L[j]+1}[j]}{(1-p_{v_k}[j])\Gamma_k[j]} & \text{otherwise} \end{cases} \tag{9}$$

where $\Gamma_k[j]$ is defined in the bottom of this page (see eq. (11)). The notations, used in (9) and (11), are defined as follows provided that vehicle is located at area $k \in \mathcal{Z}$:

- $p_{v_k}[j]$ is the internal collision probability of AC[j]. The internal collision probability can be written as

$$p_{v_k}[j] = \begin{cases} 0 & \text{for } j = 0 \\ 1 - \prod_{\ell=0}^{j-1} (1 - p_{i_k}[\ell]) & \text{otherwise} \end{cases} \tag{10}$$

- $p_{b_k}[j]$ is the back-off probability that one vehicle senses the channel as busy and hence freezes its clock, which is calculated by

$$p_{b_k}[j] = 1 - \left[\prod_{q \in S_k} (1-p_{t_q})^{N_q} \prod_{\substack{\ell=0 \\ \ell \neq j}}^{3} (1 - p_{i_k}[\ell]) \right]^{\text{AIFSN}[j]-\text{AIFSN}[0]+1}, \tag{14}$$

where S_k is the set of areas which carrier sensing ranges cover the vehicles at area k.

- $p_a[j]$ is the arrival probability of a packet of AC[j]. Since the packet generation follows a Poisson distribution, the packet arrival probability $p_a[j]$ in a time slot is given by

$$p_a[j] = 1 - \exp(-\Lambda[j] t_s), \tag{15}$$

where $\Lambda[j]$ is the packet arrival rate (packets/sec) for AC[j].

- $\rho_k[j]$ is the probability that at least one packet of AC[j] is available for transmission, which is defined by

$$\rho[j] = \Lambda[j] \times D_k[j] \tag{16}$$

where $D_k[j]$ is the average channel access delay.

We define the average channel access delay $D_k[j]$ as the average time interval from the time when a packet is available and to the time when the packet is either transmitted or dropped. By solving the Markov chain model for back-off instance, shown in [15] and after a few mathematical manipulations, $D_k[j]$ is presented in the bottom of this page (see eqns. (12) and (13)). Note that details are provided in the Appendix. So far we have a non-linear system with 147 equations (eqs. (14) and (7) to (13)) and 175 unknown variables ($p_{t_k}, p_{e_k}[j], p_{i_k}[j], p_{v_k}[j], p_{b_k}[j]$, and $D_k[j]$). To find all the unknown variables, we apply an iterative procedure presented in Algorithm 1. In the algorithm δ is a predefined

$$\Gamma_k[j] = \frac{p_{v_k}[j]\left(1-(p_{v_k}[j])^{L[j]}\right)}{1-p_{v_k}[j]} + \frac{W_0[j]-1}{2(1-p_{b_k}[j])} + \frac{1}{2(1-p_{b_k}[j])}\left[\frac{W_0[j]2p_{v_k}[j]\left(1-2^{M[j]}(p_{v_k}[j])^{M[j]}\right)}{1-p_{v_k}[j]} - \frac{p_{v_k}[j]\left(1-(p_{v_k}[j])^{M[j]}\right)}{1-p_{v_k}[j]}\right] + \frac{\left(2^{M[j]}W_0[j]-1\right)(p_{v_k}[j])^{M[j]+1}\left(1-(p_{v_k}[j])^{L[j]-M[j]}\right)}{2(1-p_{b_k}[j])(1-p_{v_k}[j])} + \frac{1-\rho_k[j]}{p_a[j]} \tag{11}$$

$$D_k[0] = T_r + \frac{\left((1-p_{b_k}[0])\sigma + (T_r + T_A[0])\,p_{b_k}[0]\right)(W_0[0]-1)}{2}. \tag{12}$$

$$D_k[j] = T_r\left(1-(p_{b_k}[j])^{L[j]+1}\right) + \frac{\left((1-p_{b_k}[j]) + (T_r+T_A[j])\,p_{b_k}[j]\right)}{2}\Bigg[(1-p_{v_k}[j])\sum_{\ell=0}^{L[j]}\Big\{(p_{v_k}[j])^{\ell}\Big(W_0[j] \times \left(2^{\min(\ell,M[j])+1}-1\right) + W_M[j]\max(0,\ell-M[j]) - \ell\Big)\Big\} + (p_{v_k}[j])^{L[j]+1} \times \Big\{W_0[j]\left(2^{\min(L[j],M[j])}-1\right) + W_M[j]\max(0,L[j]-M[j]) - L[j]\Big\}\Bigg] \quad \text{for } j = 1, 2, \text{ or } 3. \tag{13}$$

Algorithm 1 Iterative Algorithm

1: **Intialization:** Set initial values of $\rho_k[j]$ between 0 and 1 and con $= 0$.
2: **while** con $\neq 1$ **do**
3: Solve eqs. (14) and (7) to (13) to find $p_{t_k}, p_{e_k}[j], p_{i_k}[j], p_{v_k}[j], p_{b_k}[j]$, and $D_k[j]$.
4: $\rho_k^{new}[j] \leftarrow \min(1, \Lambda[j] \times D_k[j])$
5: **if** $\left|\rho_k^{new}[j] - \rho_k[j]\right| < \delta$ for $\forall k, j$ **then**
6: con $\leftarrow 1$
7: **else**
8: $\rho_k[j] \leftarrow \rho_k^{new}[j]$ for $\forall k, j$
9: **end if**
10: **end while**

threshold. After solving p_{t_k} and $D_k[j]$ from this algorithm, the numerical results on packet reception rate and average access delay are given in the following section.

V. NUMERICAL RESULTS OF BROADCASTING PERFORMANCE WITHOUT RELAYING

In this section, we present the results obtained from the analysis and validate through NS-3 simulation [26].

TABLE 5. Simulation parameters.

Parameter	Value
Bandwidth	10MHz
Data rate	6Mbps
Packet size	200 Bytes
Header duration	150 μs
Packet generation rate	10Hz
Number of vehicles	25$\sim$200
Slot time	13μs
SIFS	32μs
Retry limit	7
Simulation time	50sec
Mobility model	*Constant Position Model*
Propagation delay model	*Constant Propagation Delay Model*

A. SIMULATION SETUP AND PARAMETERS

The simulation model is based on the intersection architecture as described in Section II. A $300 \times 300\text{m}^2$ road network was considered with street width of 18m where the vehicles are uniformly distributed (generated in random locations) and vehicular mobility follows the *Constant Position Model* of NS-3. We followed the DSRC PHY and MAC layers standard [27], while part of source code of NS-3 is modified to match with the EDCA requirement presented in Section II-B and the path loss model presented in Section III. NS-3 simulation results were captured when simulation reaches in a steady state and with 95% confidence interval. Unless stated otherwise the simulation is conducted under the simulator's default setting. Along with Table 3, the additional parameters used in the simulation results are summarized in Table 5. Overall, we observe upto 5% mismatch between the simulation and analytical results, which is due to the approximation of carrier and communication ranges considered in the analysis.

B. NUMERICAL RESULTS

In the following numerical results, most of the results are presented for the case when the transmitting vehicle (V_{Tx}) broadcasts from different areas of branch A. Due to the symmetry of the intersection, presented results are also hold for the case when the transmitting vehicle broadcasts from different areas of branch B. We observe the characteristics of average access delay and packet reception probability, while varying the total number of vehicles around the intersection. Note that the total number of vehicles shown in the results does not include the transmitting vehicle.

We present the packet reception probability (PRP) while varying the total number of vehicles around the intersection. In the following, we only present the reception probability results of AC[0] packets. The reception probability of other ACs can be obtained by multiplying the reception probability of AC[0] with $1 - (p_{v_k}[j])^L$. Note that $p_{v_k}[j]$ is usually very small for moderate packet arrival rate and thus $1 - (p_{v_k}[j])^L \approx 1$. In Fig. 5, we show the impact of transmitting vehicle position on the packet reception probability (PRP) by different areas. Fig. 5a shows PRP when the transmitting vehicle broadcasts from area A_2 or A_3. It is observed that PRP at A_3 is superior compared to other areas, since no packet collision happens due to the hidden vehicles. From transmission point of view, the vehicles in area A_3 may act as hidden nodes to the vehicles of the other zones. However, from reception point of view, the receivers/vehicles of A_3 do not suffer from the hidden nodes. Although the vehicles in B_1, B_2, and B_3 areas are hidden from A_3, they do not interfere with the reception at area A_3, since their transmitted signal strength is not strong enough at area A_3 to interfere. For the other areas, PRP performance is affected by the packet collisions from hidden vehicles. Among them, PRP at G is worst since there exist highest number of hidden vehicles. When the transmitting vehicle at area A_2 or A_3, PRPs at B_1, B_2, and B_3 are always zero since the communication range of the transmitting vehicle does not reach those areas.

Fig. 5b shows the PRPs at different reception areas, provided that the transmitting vehicle broadcasts from area A_1. From the results, we observe that PRPs at A_3 and A_2 are much higher than the PRPs at G and B_1 due to the presence of hidden vehicles' packet collisions for reception at G and B_1. Among PRPs at A_3 and A_2, PRP at A_3 is slightly higher since less number of interferer vehicles for the receivers at A_3. For the same reason, PRP performance at B_1 is higher than the PRP performance at G. The PRPs at B_2 and B_3 are not plotted in Fig 5b, since they are always zero.

The PRP performances for the transmitting vehicle's position at G are plotted in Fig 5c. Note that, the PRPs at all areas are non-zero, since communication range of the transmitting vehicle covers all areas. Due to the symmetry at the intersection, PRRs at A_3 and B_3 are the same, likewise PRRs at A_1, A_2, B_1, and B_3 are the same. It is observed that for all

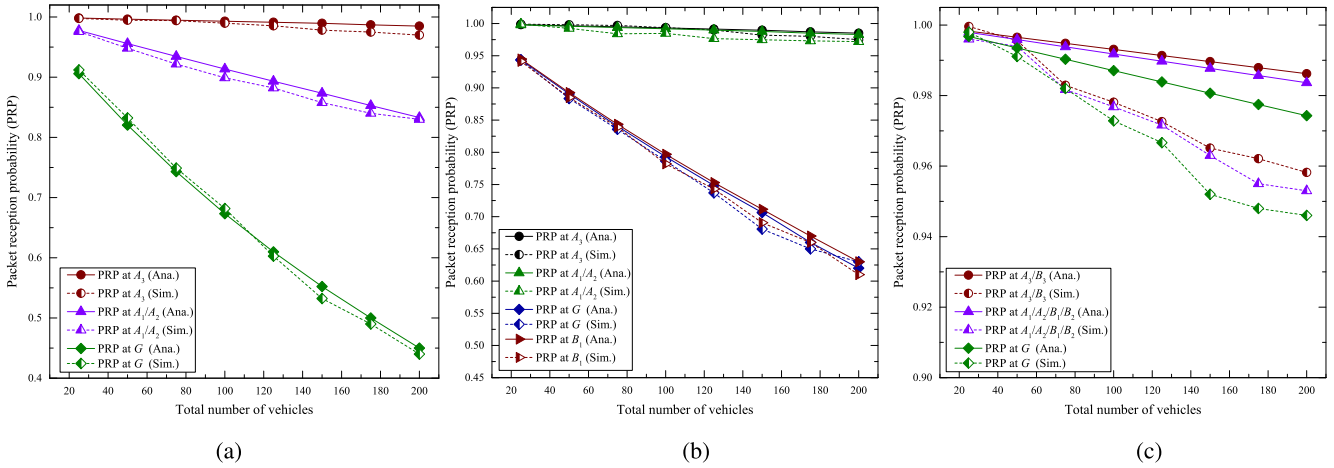

FIGURE 5. Packet reception probability at different areas of Fig. 4 while varying the location of the transmitting vehicle. (a) Transmitting vehicle located at A_2 or A_3. (b) Transmitting vehicle located at A_1. (c) Transmitting vehicle located at G.

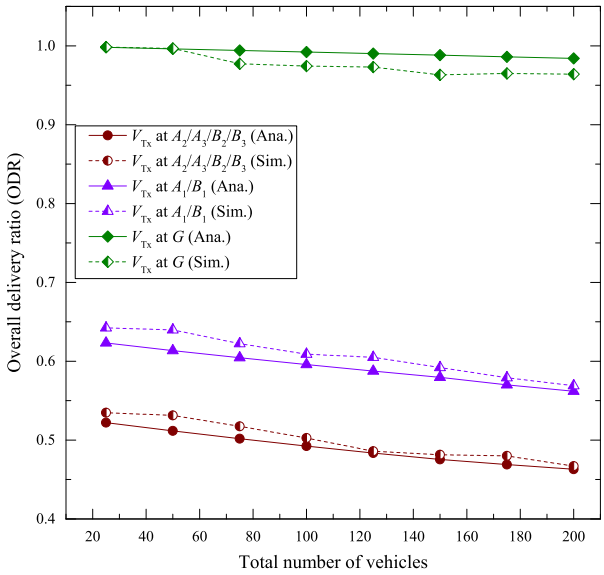

FIGURE 6. Averaged overall delivery ratio.

cases, the reception probability is over 0.9, since there exists no hidden vehicles. As expected, PRP at A_3 or B_3 is highest due to lowest number of interferer vehicles and PRP at G is lowest due to highest number of interferer vehicles.

We also present the overall packet delivery ratio ODR(x) when the transmitting vehicle broadcasts from area x. We define the overall packet delivery ratio as the ratio of average number of vehicles received the safety message to the total number of vehicles. Mathematically, The overall packet delivery ratio is calculated by the following manner:

$$\mathrm{ODR}(x) = \frac{\sum_{k \in \mathcal{Z}} \mathrm{PRP}(x,k) \times N_k}{\text{Total number of vehicles}} \tag{17}$$

The results obtained from (17) are shown in Fig 6. We notice that when the transmitting vehicle at A_1, A_2, or A_3, the delivery ratio is much less than the case when the transmitting vehicle at G. There are couple of reasons for this performance degradation: (i) the communication range of the transmitting vehicle at A_1, A_2, or A_3 is limited, (ii) severe packet collision from the hidden vehicles. When any transmission takes place from location G, the transmission will be sensed by all the vehicles. Thus, there will be no hidden vehicle for this scenario. Moreover, the vehicles at area G have the highest communication coverage due to LOS communication link with all other vehicles. Thus, when a vehicle transmits from area G, packet drops only occur when multiple vehicles start to sense the channel for transmission at the same time and then choose the same back off time instant. However, this scenario occurs very rarely due to the well-designed CSMA-CA protocol. For these reasons, we observe a superior overall delivery ratio performance when the transmitting vehicle is located at area G. We also notice that the overall packet delivery ratio does not change significantly with the variation of total number of vehicles. For a transmitting vehicle from a given area, although the PRP at few areas varies significantly with the variation of total number of vehicles, the PRP of the majority areas does not change significantly. Since the definition of overall delivery ratio takes into consideration all the areas, the impact of the former areas is neutralized by the impact of the latter areas. Hence, an insignificant change in the overall delivery ratio is observed with respect to the variation of total number of vehicles.

We now present the average channel access delay when the transmitting vehicle (V_{Tx}) broadcasts from different areas of the intersection. Fig 7 presents the average access delay of different ACs for different areas. We observe that for each area the average delay varies from lowest to highest as the priority of ACs varies from highest to lowest. This is expected due to the internal collision avoidance procedure. Among different areas, the delay for A_3 is lowest, since the transmitting vehicle can only sense the transmission from the vehicles of branch A. Thus the channel is sensed least busy

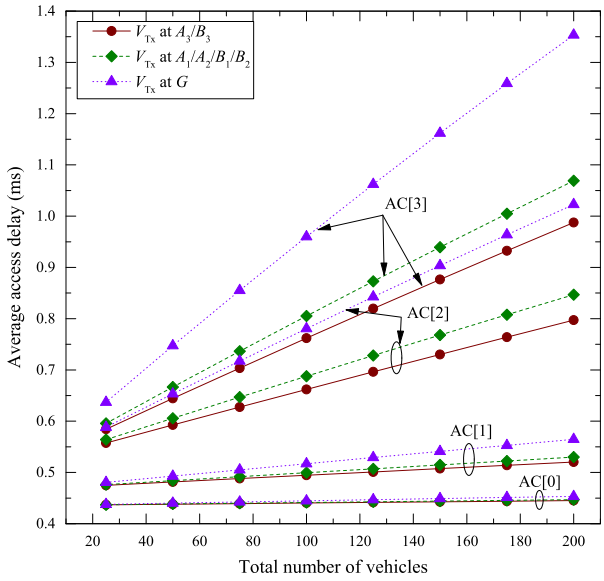

FIGURE 7. Average channel access delay of ACs for different areas of Fig. 4.

when the transmitting vehicle resides at area A_3 and the back-off counter does not need to be frozen more often. On the other hand, the access delay is highest when the transmitting vehicle at area G, since the transmitting vehicle can sense the transmission from all the vehicles around the intersection and thus, requires to freeze the back-off counter more often.

VI. IMPROVEMENT OF DELIVERY RATIO PERFORMANCE THROUGH RELAYING WITH RSU

As shown in the earlier section, the delivery ratios for the areas that are not close to the intersection are very poor. To improve the delivery ratio performance, we deploy RSU at the center of the intersection to work as a relay, which simply re-broadcasts the received safety messages. Note that retransmission is not specified in the current DSRC standard. However, it is feasible to implement the retransmission scheme in the RSU. This can be done by the following manner. Whenever the RSU correctly receives a safety message, it performs the following operation on the original message: (i) change the content of the retransmission field to indicate that the message is a retransmitted one (ii) insert a field containing the vehicle's ID, to which the message belongs (iii) insert a field to contain the original time stamp of the message i.e., the time when the message is originally generated. Whenever a vehicle receives a packet, it will check whether the packet is retransmitted or not. Since the retransmitted message will carry the MACs of both the original transmitting vehicle and the RSU, the receiving vehicle will be able to detect the transmitting vehicle. However, the retransmitted messages will have larger overhead compared to the original message. If a vehicle receives multiple replicated messages with the same transmitting vehicle ID and time stamp, it will simply discard the replicated ones.

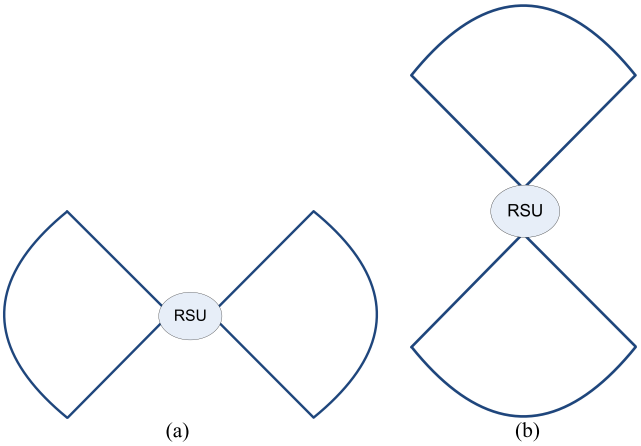

FIGURE 8. Radiation patterns of bidirectional sector antennas at RSU. (a) For branch A and C of Fig. 1. (b) For branch B and D of Fig. 1.

We consider following two antenna configurations for the RSU relaying:

- **Omni-directional antenna:** The RSU is equipped with a single omni-directional antenna. Thus the communication range, carrier sensing range, and number of interferer vehicles for the RSU are same as the other vehicles at the area G. The characteristics of the omni-directional antenna is assumed to be same as the characteristics of the antenna used in the vehicle.
- **Sector antennas:** The RSU is equipped with two special sector antennas, so called bidirectional sector antenna, where each sector antenna has same front and back radiation pattern with a beam width of $\pi/2$ rad. Thus, one sector antenna covers branch A and branch C of intersection depicted in Fig. 1, while other antenna covers branch B and branch D. The radiation patterns of these sector antennas are shown in Fig. 8. The antenna gain of each sector antenna is assumed to be same as the omni-directional antenna case and the impact of interference due to the sector antennas co-location is neglected. We consider that all the sector antennas transmit same message simultaneously. Thus, from the transmission point of view, characteristics of sector antenna configuration is identical to the omni-directional antenna configuration.

With the above configurations, the RSU can be considered as an extra vehicle at the area G. Thus, when the transmitting vehicle broadcasts from a certain area, the PRP calculation of different areas, presented in (6), needs slight modification. With a RSU at the center of the intersection, the PRP of different areas can be calculated by multiplying (6) by $(1 - p_{t_r})$, where p_{t_r} is the transmission probability of the RSU. It is obvious that, the packet generation rate at the RSU will be much higher compared to the vehicles at the streets, since the RSU requires to forward all the received safety messages. Thus the packet transmission probability of the RSU will be much higher than the transmission probability of

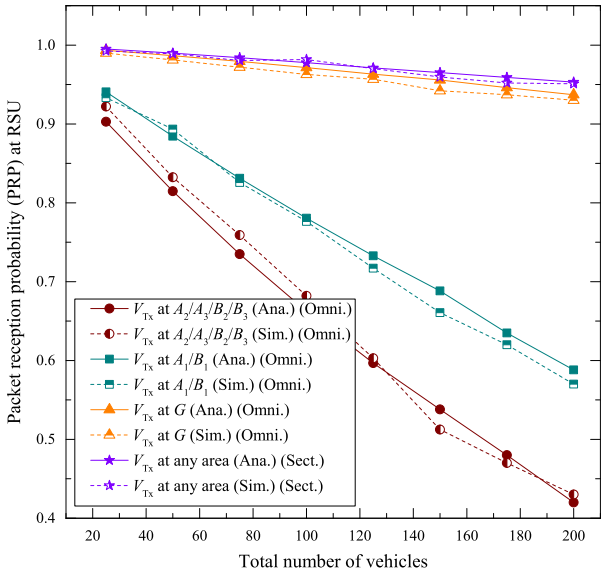

FIGURE 9. Packet reception probability at RSU with omni-directional and sector antennas.

other vehicles at area G. For simplicity, we assume saturated scenario at RSU i.e., packet of each ACs is always available at the RSU to transmit. p_{t_r} can be obtained by generating equations similar to the eqs. (14) and (7) to (10) and then by solving all the variables (variables of all area and RSU) according to the algorithm 1. Numerically it is observed that due to the addition of the RSU, the change in the transmission probability of any area is very negligible.

To find the improvement due to the RSU relaying, first we investigate the packet reception probability of the RSU. With omni-directional antenna, the PRP of RSU is same as the PRP of any other vehicle at area G. For sector antennas configuration the calculation of PRP of RSU is different. From the packet reception point of view, each sector antenna can only receive the signal from the vehicles of its designated branch and thus, simultaneous packet reception at RSU from different branches is possible. Thus, with sector antennas at RSU, the packet collision at RSU due to the hidden vehicles can be avoided. Let the transmitting vehicle is situated in any position of branch A. Hence, a successful transmission from the transmitting vehicle to the RSU is only possible when no other vehicles of branch A transmit at the time slot when transmitting vehicle broadcasts. Thus the PRP at RSU with sector antennas is independent of the position of the transmitting vehicle. The PRP of the sector antenna, that belongs to branch A, can be calculated by:

$$\mathrm{PRP}_{\mathrm{Sec}} = (1-p_{t_G})^{N_G/2} \times (1-p_{t_{A_1}})^{N_{A_1}} \times (1-p_{t_{A_2}})^{N_{A_2}} \times (1-p_{t_{A_3}})^{N_{A_3}}. \quad (18)$$

In Fig. 9, we show the packet reception probability of RSU with omni-directional and sector antennas while varying the position of the transmitting vehicle. As expected, the PRP of the RSU with omni-directional antenna is very poor when the transmitting vehicle is far away from the center of the intersection. With the sector antennas, the PRP of RSU is as high as over 0.9, regardless the position of the transmitting vehicle.

We now consider the transmission performance of the RSU. Recall that the characteristics of omni-directional or sector antennas is assumed to be same as the characteristics of antenna of a vehicle. Let $\mathrm{PRP}(r, y)$ is the packet reception probability of any vehicle at area $y \in \mathcal{Z}$ while the RSU broadcasts. $\mathrm{PRP}(r, y)$ is calculated by

$$\mathrm{PRP}(r, y) = \prod_{r \in \mathcal{I}_{G,y}} (1-p_{t_r})^{N_r}, \quad (19)$$

which is same as the PRP of different areas provided that the transmitting vehicle at area G. The results for this case is shown in Fig. 5c.

From the reception and transmission probabilities of RSU, the reception probability of different areas after relaying the safety message of the transmitting vehicle can be obtained. Let $\mathrm{RPRP}_{\mathrm{o}}(x, y)$ is the packet reception probability of any vehicle at area y provided that the transmitting vehicle first broadcasts a safety packet from area x and then the RSU with omni-directional antenna rebroadcasts that packet. In the similar fashion, we define and $\mathrm{RPRP}_{\mathrm{s}}(x, y)$ as the PRP for RSU with sector antenna relaying. We assume that if any vehicle receives a replicated message due to the relaying, it will discard the replicated one. We also assume that the RSU will re-broadcast safety message before it is expired based on the time-stamp field of each message. We calculate $\mathrm{RPRP}_{\mathrm{o}}(x, y)$ and $\mathrm{RPRP}_{\mathrm{s}}(x, y)$ by

$$\begin{aligned}\mathrm{RPRP}_{\mathrm{o}}(x, y) &= \mathrm{PRP}(x, y) \\ &\quad + (1-\mathrm{PRP}(x, y)) \times \mathrm{PRP}(G, y) \times \mathrm{PRP}(r, y), \\ \mathrm{RPRP}_{\mathrm{s}}(x, y) &= \mathrm{PRP}(x, y) \\ &\quad + (1-\mathrm{PRP}(x, y)) \times \mathrm{PRP}_{\mathrm{Sec}} \times \mathrm{PRP}(r, y).\end{aligned}$$

From the above PRPs, the overall delivery ratio after relaying can be obtained by replacing $\mathrm{PRP}(x, k)$ of (17) by $\mathrm{RPRP}_{\mathrm{o}}(x, k)$ or $\mathrm{RPRP}_{\mathrm{s}}(x, k)$. In Fig 10, we show the PRP of different areas after relaying with omnidirectional and sector antennas. For each position of the transmitting vehicle, it is observed that the PRP of any area is always better with sector antenna relaying than the PRP with omni-directional antenna relaying. Fig. 11 shows the overall delivery ratio performance with and without relaying, while the transmitting vehicle broadcasts from different areas. With relaying, a significant improvement is observed provided that the transmitting vehicle at A_1, A_2, or A_3. The performances improvements for 100 vehicles is summarized in Table 6. From the above results, we conclude that relaying through RSU can improve the delivery ratio performance of the vehicles, that are not close to the intersection. However, relaying with omni-directional antenna brings moderate improvement over the performance of the without relaying case, due to the poor reception probability of omni-directional antenna. By using sector antennas at the RSU, one can improve the reception

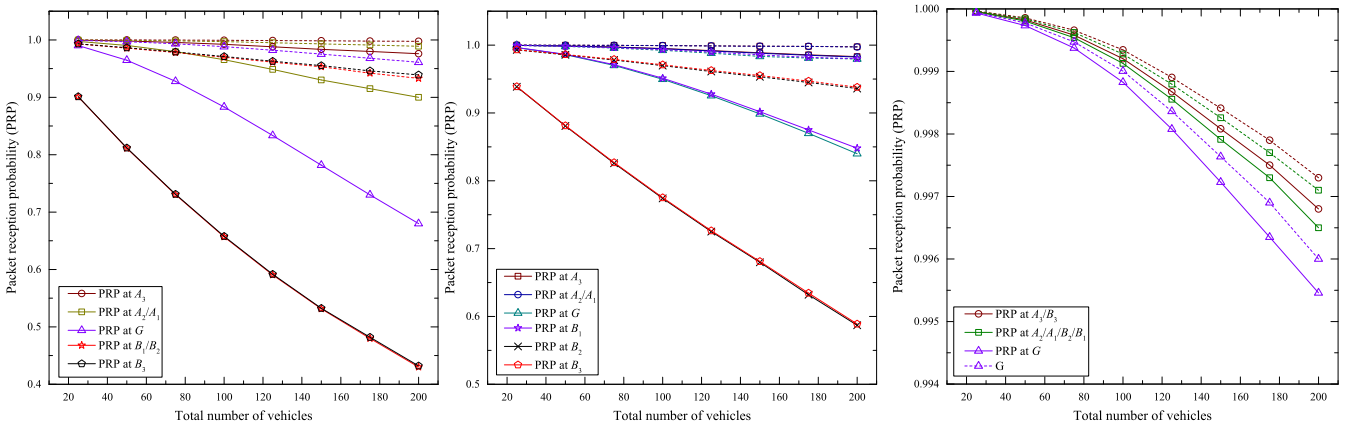

FIGURE 10. Packet reception probability of different areas after performing relaying. Solid line represents the relaying performance with omni-directional antenna, while dashed line represents the relaying performance with sector antenna. (a) Transmitting vehicle located at A_2 or A_3. (b) Transmitting vehicle located at A_1. (c) Transmitting vehicle located at G.

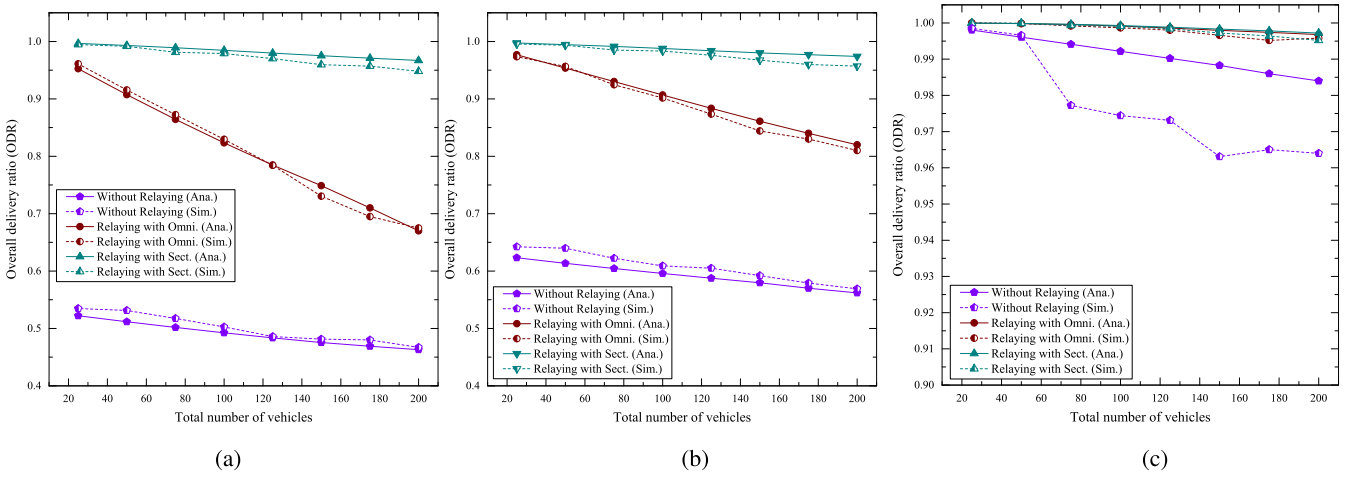

FIGURE 11. With and without relaying overall delivery ratio while varying the location of transmitting vehicle at different areas of Fig. 4. (a) Transmitting vehicle located at A_2 or A_3. (b) Transmitting vehicle located at A_1. (c) Transmitting vehicle located at G.

TABLE 6. Overall delivery ratio (ODR) improvement for 100 vehicles.

Position of V_{Tx}	ODR w/o relay	ODR with relay (omni.)	Impr. (%) over w/o relay	ODR with relay (sect.)	Impr. (%) over w/o relay
$A_2/A_3/B_2/B_3$	0.485	0.823	69.8%	0.985	103.2%
A_1/B_1	0.586	0.907	54.6%	0.988	68.4%
G	0.976	0.999	2.3%	0.999	2.3%

probability of the RSU significantly. As a result, relaying with sector antenna can improve the delivery ratio performance to a great extent.

VII. CONCLUSION

In this paper, we have investigated the performance of IEEE 802.11p safety message broadcasting at the road-intersection. Based on practical path loss model, we have partitioned the intersection in few areas to allow different communication and carrier sensing ranges for different areas. The packet reception rates of different areas are analyzed provided that the transmitting vehicle broadcasts from a certain area, and from that the overall delivery ratio is also derived. The analytical results are verified by the NS-3 simulation results, where a close match between analytical and simulation results is observed. Due to the limited communication range and collision from the hidden vehicles, it is observed that the delivery ratio is very poor when a vehicle transmits from an area that

is not close to the intersection. To improve the delivery ratio performance, we have utilized an RSU to relay the safety message. The relaying performance is analyzed by employing firstly omni-directional antenna and then special sector antennas, namely bidirectional sector antennas. From the performance comparison, it is observed that omni-directional antenna provides moderate performance improvement, while a significant performance gain can be achieved by using sector antennas.

Further works can be devoted to investigate the security concern (such as man in the middle attack) of the intersection relaying scenario. It will also be interesting to investigate the performance of IEEE 802.11p standard for the scenario, where the intersection does not have any RSU and a vehicle close to the intersection center will perform relaying (opportunistic relaying).

APPENDIX
DERIVATION OF INTERNAL TRANSMISSION PROBABILITY AND CHANNEL ACCESS DELAY

In the following analysis, we drop the notations for area for simplicity.

Internal Transmission Probability: Let $b_n[0]$ be the probability that AC[0] is in back off state $n \in \{0, W_0[0]-1\}$ and $b_{l,n}[j]$ be the probability that AC[j] ($j \in \{1,2,3\}$) is in back off state $n \in \{0, W_m[j]-1\}$ at $m^{th} \in \{0, L[j]\}$ retry event. From Markov chain analysis [15], we get the following transition probabilities:

For AC[0]:

$$b_n[0] = \frac{W_0[0]-k}{W_0[0](1-p_b[0])} b_0[0] \tag{20}$$

$$b_{\text{idle}}[0] = \frac{1-\rho[0]}{p_a[0]} b_0[0] \tag{21}$$

For AC[j] ($j \in \{1,2,3\}$):

$$b_{m,0}[j] = p_v^m[j] b_{0,0}[j] \quad m \in \{1, L[j]\} \tag{22}$$

$$b_{0,n}[j] = \frac{W_0[j]-k}{W_0[j](1-p_b[j])} b_{0,0}[j] \quad n \in \{1, W_0[j]-1\} \tag{23}$$

$$b_{m,n}[j] = \frac{(W_m[j]-k)p_v^m[j]}{W_m[j](1-p_b[j])} b_{0,0}[j] \quad n \in \{1, W_m[j]-1\}, \quad m \in \{1, L[j]\} \tag{24}$$

$$b_{m,n}[j] = \frac{(W_{M[j]}[j]-k)p_v^m[j]}{W_{M[j]}[j](1-p_b[j])} b_{0,0}[j] \quad n \in \{1, W_{M[j]}[j]-1\}, \quad m \in \{M[j]+1, L[j]\} \tag{25}$$

$$b_{\text{idle}}[j] = \frac{1-\rho[j]}{p_a[j]} b_{0,0}[j] \tag{26}$$

Recall that an AC attempts to transmit a packet as soon as the back off counter reaches at zero state. Thus, the internal transmission probability of AC[0] is $p_i[0] = b_0[0]$, while the internal transmission probability of other ACs is $p_i[j] = \sum_{m=0}^{L[j]} b_{m,0}[j] = \frac{1-(p_v[j])^{L[j]+1}}{1-p_v[j]} b_{0,0}[j]$. Since the sum of the probabilities for all states in the Markov chain is equal to one, one can find $b_0[0]$ from (20) and (21), while $b_{0,0}[j]$ can be found from (22)-(26). By substituting $b_0[0]$ and $b_{0,0}[j]$ in internal transmission probability equations, we can obtain (9) of Section IV.

Channel Access Delay: The average channel access delay of AC[j] is given by:

$$D[j] = \left. \frac{dP_{D[j]}(z)}{dz} \right|_{z=1} \tag{27}$$

where $P_{D[j]}(z)$ is the probability generating function (PGF) of channel access delay $D[j]$. Using Mason's formula on the Markov chain, $P_{D[j]}(z)$ can be obtained from following equations:

$$\begin{aligned} P_{D[0]}(z) &= \frac{T_r(z)}{W_0[0]} \sum_{n=0}^{W_0[0]-1} H[0](z), \\ P_{D[j]}(z) &= (p_v[j])^{L[j]+1} \prod_{m=0}^{L[j]} \frac{1}{W_{\min\{m,M[j]\}}[j]} \\ &\quad \times \left[\sum_{n=0}^{W_{\min\{m,M[j]\}}[j]-1} (H[j](z))^n \right] + T_r(z)(1-p_v[j]) \\ &\quad \times \sum_{i=0}^{L[j]} \left[(p_v[j])^i \left\{ \prod_{m=0}^{i} \frac{1}{W_{\min\{m,M[j]\}}[j]} \right. \right. \\ &\quad \times \left. \left. \sum_{n=0}^{W_{\min\{m,M[j]\}}[j]-1} (H[j](z))^n \right\} \right], \end{aligned} \tag{28}$$

where $T_r(z)$ is the PGF of transmission time and $H[j](z)$ is the PGF of the time that the back off counter of ACj decremented by one, which is defined by,

$$H[j](z) = (1-p_b[j])z^{t_s} + p_b[j]z^{T_r+T_A[j]}. \tag{29}$$

Recall that t_s is the duration of a time slot and $T_A[j] = \text{SIFS} + \text{AIFSN}[j] \times t_s$. By substituting $P_{D[0]}(z)$ and $P_{D[j]}(z)$ (for $j \in \{1,2,3\}$) in (27), we can obtain (12) and (13) of Section IV.

REFERENCES

[1] *IEEE Standard for Infor Mation Technology–Local and Metropolitan Area Networks–Specific Requirements–Part 11: Wireless LAN Medium Access Control (MAC) and Physical Layer (PHY) Specifications Amendment 6: Wireless Access in Vehicular Environments*, IEEE Standard 802.11, Jul. 2010, pp. 1–51.

[2] *Intelligent Transport Systems (ITS); Vehicular Communications; Basic Set of Applications; Part 2: Specification of Cooperative Awareness Basic Service*, ETSI Standard Rev. V1.3.0 Draft, 2013.

[3] "Dedicated short range communications (DSRC) message set dictionary," SAE Tech. Paper J2735, 2009. [Online]. Available: https://www.sae.org/standards/content/j2735_200911/

[4] X. Li, T. D. Nguyen, and R. P. Martin, "An analytic model predicting the optimal range for maximizing 1-hop broadcast coverage in dense wireless networks," in *Proc. 3rd Int. Conf. Ad-Hoc, Mobile, Wireless Netw. (ADHOC-NOW)*, Vancouver, Canada, Jul. 2004, pp. 172–182.

[5] Z.-N. Kong, D. H. K. Tsang, B. Bensaou, and D. Gao, "Performance analysis of IEEE 802.11e contention-based channel access," *IEEE J. Sel. Areas Commun.*, vol. 22, no. 10, pp. 2095–2106, Dec. 2004.

[6] H. Wu, X. Wang, Q. Zhang, and X. Shen, "IEEE 802.11e enhanced distributed channel access (EDCA) throughput analysis," in *Proc. IEEE Int. Conf. Commun.*, vol. 1. Jun. 2006, pp. 223–228.

[7] Z. Tao and S. Panwar, "Throughput and delay analysis for the IEEE 802.11e enhanced distributed channel access," *IEEE Trans. Commun.*, vol. 54, no. 4, pp. 596–603, Apr. 2006.

[8] C. L. Huang and W. Liao, "Throughput and delay performance of IEEE 802.11e enhanced distributed channel access (EDCA) under saturation condition," *IEEE Trans. Wireless Commun.*, vol. 6, no. 1, pp. 136–145, Jan. 2007.

[9] I. Inan, F. Keceli, and E. Ayanoglu, "Analysis of the 802.11e enhanced distributed channel access function," *IEEE Trans. Commun.*, vol. 57, no. 6, pp. 1753–1764, Jun. 2009.

[10] F. Kaabi, P. Cataldi, F. Filali, and C. Bonnet, "Performance analysis of IEEE 802.11p control channel," in *Proc. 6th Int. Conf. Mobile Ad-Hoc Sensor Netw.*, Dec. 2010, pp. 211–214.

[11] S. Eichler, "Performance evaluation of the IEEE 802.11p WAVE communication standard," in *Proc. IEEE Veh. Technol. Conf.*, Oct. 2007, pp. 2199–2203.

[12] J. R. Gallardo, D. Makrakis, and H. T. Mouftah, "Mathematical analysis of EDCA's performance on the control channel of an IEEE 802.11p WAVE vehicular network," *EURASIP J. Wireless Commun. Netw.*, vol. 2010, no. 1, p. 489527, Apr. 2010. [Online]. Available: http://dx.doi.org/10.1155/2010/489527

[13] C. Han, M. Dianati, R. Tafazolli, R. Kernchen, and X. Shen, "Analytical study of the IEEE 802.11p MAC sublayer in vehicular networks," *IEEE Trans. Intell. Transp. Syst.*, vol. 13, no. 2, pp. 873–886, Jun. 2012.

[14] K. A. Hafeez, L. Zhao, B. Ma, and J. W. Mark, "Performance analysis and enhancement of the DSRC for VANET's safety applications," *IEEE Trans. Veh. Technol.*, vol. 62, no. 7, pp. 3069–3083, Sep. 2013.

[15] Y. Yao, L. Rao, and X. Liu, "Performance and reliability analysis of IEEE 802.11p safety communication in a highway environment," *IEEE Trans. Veh. Technol.*, vol. 62, no. 9, pp. 4198–4212, Nov. 2013.

[16] J. Zheng and Q. Wu, "Performance modeling and analysis of the IEEE 802.11p EDCA mechanism for VANET," *IEEE Trans. Veh. Technol.*, vol. 65, no. 4, pp. 2673–2687, Apr. 2016.

[17] H. Peng *et al.*, "Performance analysis of IEEE 802.11p dcf for multiplatooning communications with autonomous vehicles," *IEEE Trans. Veh. Technol.*, vol. 66, no. 3, pp. 2485–2498, Mar. 2017.

[18] H. Cheng and Y. Yamao, "Reliable inter-vehicle broadcast communication with sectorized roadside relay station," in *Proc. IEEE 77th Veh. Technol. Conf. (VTC Spring)*, Jun. 2013, pp. 1–5.

[19] X. Ma, M. Wilson, X. Yin, and K. S. Trivedi, "Performance of VANET safety message broadcast at rural intersections," in *Proc. Int. Wireless Commun. Mobile Comput. Conf. (IWCMC)*, Jul. 2013, pp. 1617–1622.

[20] L. T. Trien and Y. Yamao, "An investigation of network coding relay in its V2V communication at intersections," in *Proc. IEEE Int. Conf. Netw. Infrastruct. Digit. Content*, Sep. 2014, pp. 297–301.

[21] X. Ma, G. Butron, and K. Trivedi, "Modeling of VANET for BSM safety messaging at intersections with non-homogeneous node distribution," in *Proc. Int. Workshop Commun. Technol. Vehicles*, San Sebastián, Spain, Jun. 2016, pp. 149–162.

[22] T. S. Kim, H. Lim, and J. C. Hou, "Understanding and improving the spatial reuse in multihop wireless networks," *IEEE Trans. Mobile Comput.*, vol. 7, no. 10, pp. 1200–1212, Oct. 2008.

[23] T. Mangel, O. Klemp, and H. Hartenstein, "5.9 GHz inter-vehicle communication at intersections: A validated non-line-of-sight path-loss and fading model," *EURASIP J. Wireless Commun. Netw.*, vol. 2011, p. 182, Dec. 2011.

[24] L. Cheng, B. E. Henty, D. D. Stancil, F. Bai, and P. Mudalige, "Mobile vehicle-to-vehicle narrow-band channel measurement and characterization of the 5.9 GHz dedicated short range communication (DSRC) frequency band," *IEEE J. Sel. Areas Commun.*, vol. 25, no. 8, pp. 1501–1516, Oct. 2007.

[25] T. Abbas and K. Sjöberg, J. Karedal, and F. Tufvesson, "A measurement based shadow fading model for vehicle-to-vehicle network simulations," *Int. J. Antennas Propag.*, vol. 2015, May 2015, Art. no. 190607.

[26] ns-3. *A Discrete-Event Network Simulator*. Accessed: Nov. 25, 2017. [Online]. Available: https://www.nsnam.org/

[27] J. B. Kenney, "Dedicated short-range communications (DSRC) standards in the United States," *Proc. IEEE*, vol. 99, no. 7, pp. 1162–1182, Jul. 2011.

MD. NOOR-A-RAHIM received the Ph.D. degree in telecommunications from the Institute for Telecommunications Research, University of South Australia, Australia, in 2015. He is currently a Research Fellow with the Centre for Infocomm Technology, Nanyang Technological University, Singapore. His research interests include information theory, wireless communications, and vehicular communications. He was a recipient of the Michael Miller Medal for the most outstanding Ph.D. thesis in 2015 from the Institute for Telecommunications Research, University of South Australia.

G. G. MD. NAWAZ ALI received the B.Sc. degree from the Department of Computer Science and Engineering, Khulna University of Engineering and Technology, Bangladesh, in 2006, and the Ph.D. degree from the Department of Computer Science, City University of Hong Kong, in 2013. He was a Researcher with the City University of Hong Kong for a while. He joined the Khulna University of Engineering and Technology as an Assistant Professor. He was a Post-Doctoral Research Fellow with the School of Electrical and Electronic Engineering, Nanyang Technological University, Singapore 2015. He is currently a Post-Doctoral Research Fellow with the Department of Automotive Engineering, Clemson University, USA. His current research interests include network coding, wireless broadcasting, mobile computing, and ad hoc networking with a focus on vehicular ad hoc networking. He is a reviewer of a number of international journals including the IEEE TRANSACTIONS ON INTELLIGENT TRANSPORTATION SYSTEMS, the *IEEE Transactions on Intelligent Transportation Systems Magazine*, the IEEE TRANSACTIONS ON VEHICULAR TECHNOLOGY, and *Wireless Networks*. He is a member of IEEE VTS.

HIEU NGUYEN received the Ph.D. degree in electronics engineering from Chungbuk National University, South Korea, in 2007. He is currently a Research Fellow with the School of Electrical and Electronic Engineering, Nanyang Technological University, Singapore. His major research interests are signal processing for communications, multicarrier and multiple-antenna systems, and vehicular communications.

YONG LIANG GUAN is currently a tenured Associate Professor with the School of Electrical and Electronic Engineering, Nanyang Technological University, Singapore. He has published an invited monograph, three book chapters, and over 300 journal and conference papers. He has led 13 past and present externally funded research projects on advanced wireless communication techniques, coding for 10 Tbits/in^2 magnetic recording, and acoustic telemetry for drilling application, with total funding over SGD 9 million. His research interests broadly include coding, signal design and signal processing for communication systems, storage systems, and information security systems. He is the Chair of the IEEE ComSoc Singapore Chapter. He was an Associate Editor of the IEEE SIGNAL PROCESSING LETTER. He is an Associate Editor of the IEEE TRANSACTIONS ON VEHICULAR TECHNOLOGY.